Systems Microbiology and Biomanufacturing (2026) 6:133
https://doi.org/10.1007/s43393-026-00539-4

RESEARCH

Yeast-derived biomolecule mixtures from wine lees display antimicrobial activity: an integrated bioprocess approach against grapevine pathogens

Artemis Tsioka[1] · Pol Gimenez-Gil[1] · Angeliki Kasioura[1] · Aikaterini Tzamourani[1] · George Ntourtoglou[1] · Konstantina Ploumpi[1] · Alexandra Evangelou[1] · Christina Virgiliou[2,3] · Georgios Theodoridis[2,3] · Maria Dimopoulou[1] · Panagiotis Arapitsas[1,4] · Danai Gkizi[1]

Received: 15 May 2026 / Revised: 10 July 2026 / Accepted: 14 July 2026

Abstract

Grapevine trunk diseases threaten sustainable viticulture, while wine lees remain an underexploited biocontrol-relevant by-product within the circular economy framework. An integrated bioprocess was developed to upgrade lees into high-molecular-weight biomolecule mixtures and low-molecular-weight peptide-enriched fractions through a defined sequence of unit operations: fermentation design by using *Saccharomyces* monocultures and sequential inoculations with non-*Saccharomyces* strains, ultrasound-assisted autolysis, enzymatic hydrolysis, and 3 kDa ultrafiltration. The antifungal activity of the products was tested *in vitro* and *in vivo* against *Phaeomoniella chlamydospora* and *Phaeoacremonium minimum*, the two main pathogens that cause Petri disease in grapevine. The results demonstrated that high-molecular-weight autolysates showed no inhibition. The post-hydrolysis fractions reduced mycelial growth of *Phaeoacremonium minimum* by 45%–75% and *Phaeomoniella chlamydospora* by 40%–57%, and decreased conidiation by up to 92% and 61%, respectively. They also reduced symptoms (wood discoloration) by 47%–52% and 35%–73% and endophytic fungal growth by 63%–84% and 80%–91% respectively. Those results indicate an association between hydrolysis and the appearance of antifungal activity. Untargeted metabolomics employing liquid chromatography–mass spectrometry (UHPLC–ESI–TIMS–QTOF) highlighted strain- and fermentation-dependent secondary metabolite signatures, with 448 features differentiating across fermentation conditions. Activity-based correlation fingerprinting identified 49 putative biomarkers negatively associated with pathogen growth. Overall, fermentation design functions as a controllable upstream quality parameter, offering a scalable circular economy pathway for the production of antifungal bioproducts derived from winery waste.

Highlights

- Wine lees were converted into peptide-enriched mixtures by bioprocessing.
- Hydrolyzed fractions inhibited two grapevine trunk disease pathogens.
- LC–MS revealed yeast-dependent low-molecular-weight signatures.

Keywords Antimicrobial biomolecule mixtures · Enzymatic hydrolysis · Peptide enriched mixtures · Grapevine phytoprotection · Metabolomics · Wine lees valorization

Artemis Tsioka and Pol Gimenez-Gil have contributed equally to this work.

✉ Maria Dimopoulou
mdimopoulou@uniwa.gr

✉ Panagiotis Arapitsas
panagiotis.arapitsas@fmach.it

[1] Department of Wine, Vine and Beverage Sciences, School of Food Sciences, University of West Attica, Athens 12243, Greece

[2] Biomic AUTh, Center for Interdisciplinary Research and Innovation (CIRI-AUTH), Balkan Center B1.4, 10th km Thessaloniki-Thermi Rd, Thessaloniki 57001, Greece

[3] AUTh Node, Center for Interdisciplinary Research and Innovation (CIRI-AUTH), FoodOmicsGR Research Infrastructure, Thessaloniki 57001, Greece

[4] Research and Innovation Centre, Fondazione Edmund Mach, Trento 38010, Italy

Published online: 12 August 2026

Introduction

Wine lees, the sediment formed at the bottom of the fermentation tank or barrels, represent the second major winery by-product, accounting for about 25% (De Iseppi et al. 2020). They are mainly composed of dead and alive yeast cells, containing proteins and peptides, polysaccharides, lipids, polyphenols, and their composition depends on numerous parameters, like the yeast species/strains and the grape cultivars (Bordiga 2016; De Iseppi et al. 2020; Niculescu and Ionete 2023). Due to high oxygen demand (Pons-Mercadé et al. 2021) and various insoluble particles, lees are considered environmental pollutants, making their disposal costly for the wine industry. Given the global interest on innovative processing for value-addition, the development of efficient strategies for the recovery of high-value compounds from winemaking by-products is a critical priority for the agri-food industry. Wine lees represent a high-potential winery side-stream for the development of natural antimicrobial solutions, enriched in bioactive substances such as peptides and metabolites possibly useful for the control of plant pathogens, through engineered bioprocessing. The bioactivity of microbial metabolites and their antimicrobial properties have been extensively studied for years (Bérdy 2005) as well as their use in phytoprotection (Das et al. 2026). Several small peptides and proteins are also well-known for their activity against microorganisms, oxidative reactions, enhancing plant immune system, etc. (Marcos et al. 2008). Oligopeptides, usually formed by 2–50 amino acid residues, can exhibit different biological functions, and they may exist as an independent entity or be produced after hydrolysis from the parent protein (Akbarian et al. 2022). The bioactivity of peptides is critically dependent on their physicochemical properties, including net positive charge (Mookherjee and Hancock 2007), amphipathicity (Chen et al. 2021), hydrophobicity (Allen and Pellois 2022), steric hindrance (Sagan et al. 2003) and specific structural motifs (Brango-vanegas et al. 2024) that enable interactions with fungal cell components.

The use of peptides with antimicrobial activity for the control of plant pathogens is a new trend in plant pathology with promising results. Peptides isolated by microorganisms have demonstrated to exhibit functions against powdery mildew (Romero et al. 2007; Sanchez-Vallet et al. 2010), downy mildew (Deravel et al. 2014; Colombo et al. 2020), and bunch rot (Zhang et al. 2018) *in vivo*. The possibility of using bioactive compounds of wine lees for the control of grapevine trunk pathogens, to the best of our knowledge, has never been taken into consideration previously.

Against this background, particular attention has been directed to *Phaeomoniella chlamydospora* and *Phaeoacremonium minimum*, two ascomycetes fungi associated with Petri disease, one of the most severe Grapevine Trunk Diseases (GTDs), which affects young grapevines. They colonize the wood tissue, causing wood discoloration by the appearance of brown striking, wood necrosis, "tiger stripes" on leaves, stunted growth, wilting, apoplexy or even the death of the plant (Gramaje et al. 2018). Petri disease lacks effective chemical control measures, especially since the ban of sodium arsenite due to its risks to human health (del Pilar Martínez-Diz et al. 2021), making biocontrol strategies an attractive alternative solution.

This work provides a multidisciplinary approach to assessing whether industrial wine lees can be converted into bioactive mixtures through a defined, controllable bioprocessing and downstream fractionation strategy, offering a novel solution for the agri-food sector. The central hypothesis is that controlled fermentation schemes, yeast autolysis, and protein hydrolysis would release bioactive molecules, such as peptides, capable of inhibiting fungal growth and reducing symptoms caused by the pathogens. To test this, mixed and monoculture fermentations, using selected oenological yeasts, were carried out to generate lees with distinct biochemical profiles. From these, high- and low-molecular-weight biomolecule mixtures (HMW-BM and LMW-BM) were prepared and evaluated *in vitro* and *in vivo* for antifungal and phytoprotective activity. Finally, untargeted metabolomics was employed to characterize the chemical fingerprint of the most active mixtures. The experimental design is illustrated in Fig. 1.

Materials and methods

Wine lees production

Yeast strains and pre-cultures

This study employed two *Saccharomyces cerevisiae* strains, a newly isolated indigenous strain (S1) (Tzamourani et al. 2023) and a commercial strain (S3), along with a commercial *Hanseniaspora* sp. strain (H), known to enhance aromatic complexity in mixed cultures with *S. cerevisiae* (Tzamourani et al. 2026).The strains were preserved at -20 °C in Yeast Peptone Dextrose (YPD) broth [g/L: 10 yeast extract (Condalab, Spain), 10 bacteriological peptone (Condalab, Spain), 20 dextrose (Merck, Germany)] supplemented with 30% glycerol (Merck, Germany). Before starting the experiments, the cultures were incubated twice on YPD agar [g/L: 10 yeast extract (Condalab, Spain), 10 bacteriological peptone (Condalab, Spain), 20 dextrose (Merck, Germany), 20 agar (Condalab, Spain)] at 28 °C for 48 h. The precultures were used to inoculate fermentation.

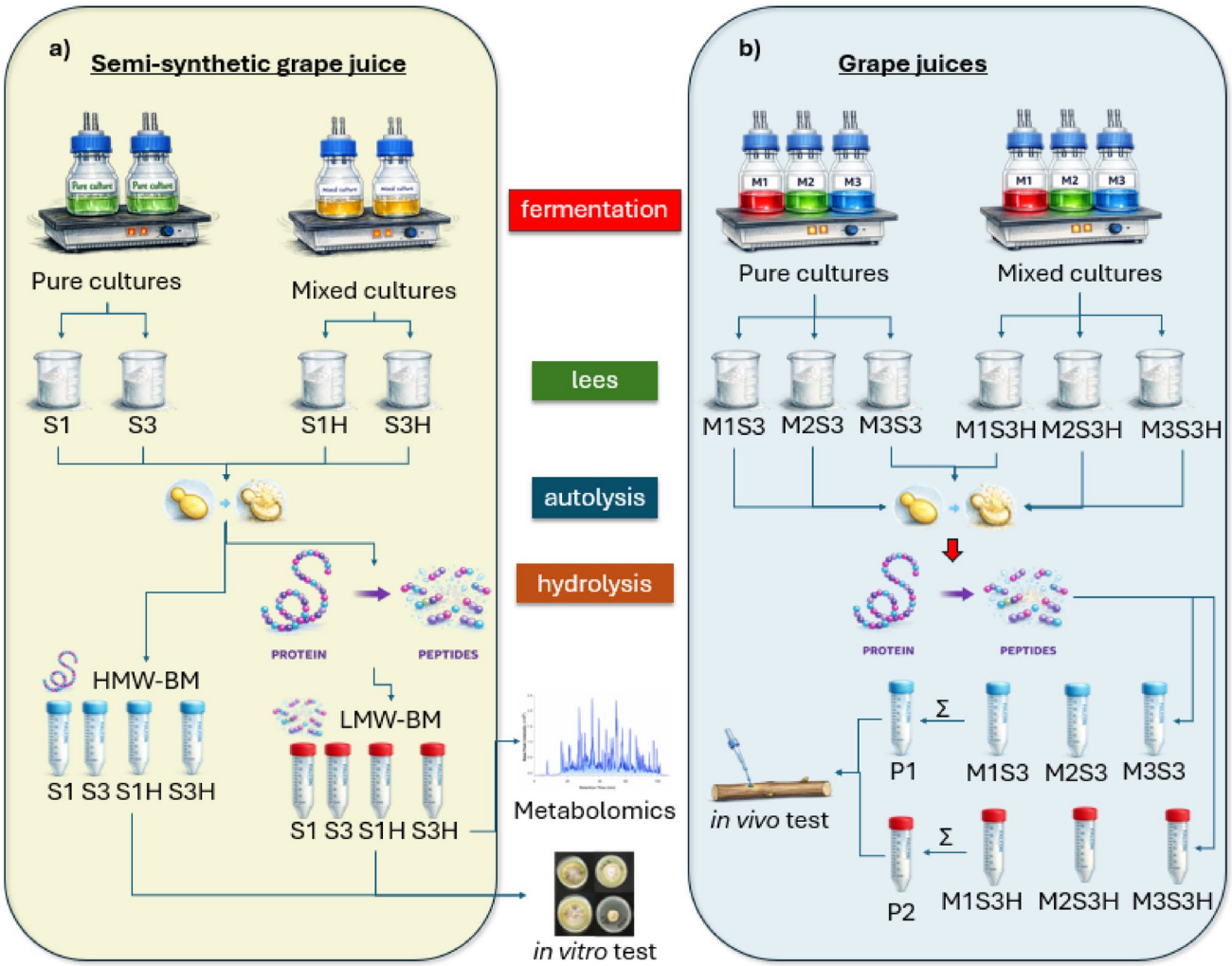

Fig. 1 Graphical illustration of experimental design for *in vitro* assays (**a**) and *in vivo* assays (**b**). S1, S3: products obtained from monoculture fermentation with *Saccharomyces cerevisiae* strain S1 and S3, respectively, S1H, S3H: products obtained from mixed cultures fermentation with strain S1 and *Hanseniaspora* sp. strain H, and *Saccharomyces cerevisiae* strain S3 and *Hanseniaspora* sp. strain H, respectively, HMW-BM: High Molecular Weight Biomolecule mixtures, LMW-BM: Low Molecular Weight Biomolecule mixtures, M1S3, M2S3, M3S3: products obtained from monoculture fermentation with *Saccharomyces cerevisiae* strain S3 in musts M1, M2 and M3, respectively, M1S3H, M2S3H, M3S3H: products obtained from mixed cultures fermentation with strain S3 and *Hanseniaspora* sp. strain H in musts M1, M2 and M3, respectively, P1: product resulted from mixing of products M1S3, M2S3, M3S3, P2: product resulted from mixing of products M1S3H, M2S3H, M3S3H

Fermentation medium

The mixtures used for the *in vitro* assays were produced from wine lees created by fermentation in a laboratory grape juice medium that simulated wine conditions. The medium contained 250 mL/L white grape must, 5 g/L yeast extract (Condalab, Spain), 1 mL/L Tween 80 (Merck, Germany) and final total sugar concentration of 180 g/L [90 g/L *D*-glucose (Merck, Germany) and 90 g/L *D*-fructose (Merck, Germany)]. Prior to yeast inoculation, the grape juice medium (GJ) was sterilized by filtration using a 0.45 µm nitrate cellulose membrane (Millipore, Molsheim, France). Consequently, the effectiveness of sterilization was verified by plate counting in YPD agar (28 °C for 48 h). Microbiological analysis of the filtered grape juice confirmed the absence of viable, culturable cells, indicating effective sterilization. For *in vivo* assays the medium for fermentation was grape must. Three different monovarietal grape musts of Greek varieties were used: (i) Savatiano (M1) from the region of Attica, Greece, (ii) Roditis (M2) and (iii) Moschofilero (M3), from the region of Nemea, Greece. The use of three different grape musts in the *in vivo* experiments aimed to minimize the impact of grape variety on the metabolites production in the resulting wine lees. The resultant products were named M1S3, M2S3, M3S3, each produced from a different must produced via separate monoculture fermentation schemes,

and M1S3H, M2S3H, M3S3H, each produced from a different must via mixed culture fermentation schemes.

Fermentation assays

Triplicate experiments were carried out in sterile Duran bottles at 18 °C under slight orbital spinning conditions (150 r/min) in order to mimic the thermodynamic forces that generate rotational motion of the medium under industrial conditions (Rollero et al. 2018). Four different modalities were conducted to create the mixtures for the *in vitro* experiments: (i) pure culture of S1 (ii) pure culture of S3, (iii) a sequential mixed modality, where H strain was inoculated 48 h before S1, and (iv) H strain was inoculated 48 h before S3. Two modalities were conducted to create the mixtures for the *in vivo* experiments: i) pure culture of S3, iii) a sequential mixed modality, where H strain was inoculated 48 h before S3. In all trials, both the single and mixed cultures were inoculated at a concentration of 1×10^6 viable cells/mL. In Online Resource ESM_1, Table S1 illustrates the coding of inoculation modalities. The musts were microbiologically analyzed by aseptically plate spreading 0.5 mL of the sample on YPD agar prior to inoculation, and no culturable colonies were detected. Fermentations took place under slight orbital spinning conditions. Fermentations' kinetics were monitored by weighing the bioreactors twice daily or more. After the completion of fermentation processing, all the quantity of the fermented products from each fermentor was centrifuged at 5,000 × *g* for 10 min. The yeast biomass was then washed once with Ringer's solution (Merck, Germany), and all biomass was aseptically collected in sterile 50 mL Falcon tubes. Biomass was determined based on wet weight measurements.

Population dynamics

Samples were collected at 0, 24, 48, 72, 96, and 192 h throughout the fermentation process, and the recovered lees were subsequently subjected to classical microbiological analysis. Briefly, the samples were serially diluted in tenfold steps, and appropriate dilutions were plated onto the corresponding culture media. Yeast growth in monocultures was assessed by plating onto YPD agar medium and incubating at 28 °C for 48 h before colony enumeration (expressed as CFU/mL). For sequential inoculation experiments, yeast growth was monitored using two different agar media substrates: (a) YPD agar and (b) Wallerstein Laboratory Nutrient Agar (WL) (Condalab, Spain), enabling differentiation between *S. cerevisiae* and *Hanseniaspora* sp. On WL agar, after 72 h of incubation at 28 °C, *S. cerevisiae* colonies appeared white, while *Hanseniaspora* sp. colonies developed a blue coloration. All data correspond to the average values recovered from triplicate fermentations and duplicated analysis. Population dynamics and biomass production were visualized in GraphPad Prism 5 software.

Yeast autolysis and determination of total protein content of HMW-BM mixtures

Biomass samples were centrifuged at 1,500 r/min at room temperature using 50 mL Falcon tubes. The solid fraction obtained after centrifugation was subjected to ultrasound treatment, employing a 1:1 dilution ratio in lysis buffer (Tris-HCl 50 mmol/L, NaCl 150 mmol/L, EDTA 1 mmol/L and Triton X-100 0.05% (Merck, Germany) combined with a 15-minute ultrasound optimized protocol at room temperature (Ntourtoglou et al. 2025). Following the autolysis process, the autolysates were centrifuged again, and the protein content was determined based on the Bradford method (Bradford 1976), using Quick Start™ Bradford Protein Assay Kit (Bio-Rad). In brief, samples were first diluted 1:4 with deionized water and volumes of 20 µL were added over 1mL of Bradford Dye Reagent, previously warmed to room temperature. Samples were incubated at room temperature for 5 min, and then the absorbance was read at 595 nm. The protein content, *C* (mg/L), was estimated based on a calibration curve, using Bovine Serum Albumin (BSA) (Merck, Germany) as a standard protein ($y = 0.0011x + 0.1207$, $R^2 = 0.9958$) (Online Resource ESM_1, Table S1). Based on total biomass input, approximately 2 mg protein was recovered per gram of biomass. The resulting products consisted of the HMW-BM mixtures, and were subsequently divided into two parts: (a) one used for the *in vitro* experiments (HMW-BM- S1, S3, S1H and S3H), and (b) one used for protein hydrolysis to produce the LMW-BM mixtures, which were also used in the *in vitro* assays.

Protein hydrolysis and delivery of low-molecular-weight bioactive fractions" (LMW-BM mixtures)

For the enzymatic hydrolysis of proteins contained in HMW-BM mixtures, samples were first diluted in 1:2 ratio with deionized water. The enzyme Flavourzyme® (500 U/g, $d = 1.1$ g/mL, Merck, Germany) was used at a concentration of 44 LAPU/mg of protein, for 2 h stirring at pH 5. The enzyme was deactivated by adding 6 mol/L HCl until the pH was below 3. The solution was centrifuged to remove solid particles. Ultrafiltration of the supernatant was followed, with 3 kDa MW cut-off value membrane (Amicon® Ultra-15 3 K, Millipore), to obtain products of low

molecular weight, rich in peptides. The concentration of free alpha-amino nitrogen (FAN, mg N_2/L) in the supernatant of these mixtures, was measured using an automatic enzymatic analyzer (Hyperlab Smart, Steroglass), based on NOPA method (Dukes and Butzke 1998) (Online Resource ESM_1, Table S1). The resultant LMW products tested *in vitro* were LMW-BM-S1, S3, S1H, and S3H. For *in vivo* tests, the LMW products used were P1 and P2. P1 was produced by mixing three LMW products (M1S3, M2S3, M3S3), each originating from a different must produced via separate monoculture fermentation schemes. P2 was produced by mixing three LMW products (M1S3H, M2S3H, M3S3H), each from a different must produced via mixed culture fermentation schemes. The proportion of all products was 1:1:1.

Preparation of microbial inoculum for inhibition assays

The fungal strains used for the *in vitro* experiments, *Pm. minimum* and *Pa. chlamydospora* (Gkikas et al. 2021), were previously isolated from infected grapevine wood and belong to the microbial collection of the Laboratory of Plant Pathology of the Agricultural University of Athens. The fungi were grown on Petri dishes containing Potato Dextrose Agar (PDA) (Merck, Germany) at 24 °C for 18 days in the dark.

In vitro evaluation for fungal growth and conidia production

HMW-BM and LMW-BM mixtures were evaluated for their *in vitro* ability to reduce the growth and sporulation of *Pm. minimum* and *Pa. chlamydospora.* Considering similar studies in the literature (Jang et al. 2006; Sun et al. 2022) preliminary experiments have been conducted to test the effectiveness of two concentrations, 10 and 20 µg/mL, of each of the HMW-BM and LMW-BM mixtures, to identify the most effective low concentration (data are not shown). Since at the concentration of 20 µg/mL there was total inhibition of the mycelium growth and no differences were observed, the concentration of 10 µg/mL has been selected for the following experiments.

The effectiveness of HMW-BM and LMW-BM mixtures was evaluated in PDA (Merck, Germany) growth medium amended with 10 µg/mL of each biomolecule mixture individually. The same procedure was followed for both fungi. In brief, an agar plug from an actively growing colony of the fungus on PDA was placed in the center of a petri dish (5.2 cm diameter). The dishes were placed in the dark at 24 °C and the diameter (cm) of the fungal growth was recorded at 18 days post inoculation (dpi). For sporulation measurements, the edge of the fully grown fungal culture was cut with a cork borer (6 mm diameter) and vortexed three times, for 30 s each time, in 1mL sterilized distilled H_2O. Sporulation of both fungi was assessed under a light microscope by using a Neubauer counting chamber and expressed relative to the conidiation in the control treatment, which was set at 100% (Tsioka et al. 2024). The sporulation of the fungi in the presence of the evaluated products was assessed at 18 dpi. All biomolecule mixtures were tested in triplicates (3 petri dishes) and the experiment was repeated three times ($n=9$).

In vivo evaluation for phytoprotective effect

Products P1 and P2 were evaluated for their phytoprotective effect *in vivo* Detached canes (≈25 cm) with three buds, from Syrah cultivar, were surface sterilized by immersing them for 10 min in 10% chloride solution, 5 min in 70% ethanol solution and rinsed 5 min in sterilized water. Subsequently, rooting hormone powder (indolylbutyric acid 0.25%, Radicin, Phytorgan) was applied to canes before they were placed for rooting in autoclaved soil amended with 25% perlite, in a controlled conditioning chamber of 25 °C and a photoperiod of 14 h of light and 10 h of darkness. Three weeks later, 650 mL of products P1 and P2 with a concentration of 10 µg/mL of each biomolecule mixture individually, were applied in soil. For control, sterilized, distilled water was used. One week after the products application, a 2 mm hole was opened in artificially inoculated rooted cuttings and 20 µL of conidia suspension (1×10^8 conidia/mL) of *Pm. minimum* or *Pa. chlamydospora* were inoculated inside the hole. Artificially inoculated rooted cuttings were incubated in the chamber for 4 months. For control, 20 µL Potato Dextrose Broth (PDB) was placed in the hole instead of conidia. Measurements of the wood discoloration caused by the two pathogens, were conducted at 112 dpi. Wood tissue 1 cm around the inoculation point was also collected at 112 dpi for endophytic fungal DNA, lignin, and phenolic compounds quantification.

Endophytic fungal DNA relative quantification using Real time PCR

For the endophytic relative quantification of the fungal DNA, wood tissue from 1 cm around the inoculation point was pulverized in the presence of liquid nitrogen. DNA isolation from wood around the inoculation point was conducted according to Christopoulou et al. (2024). DNA concentration was measured by using a NanoView Photometer (FastGene, Model: FG-NP02). The primers used for the quantification of *Pm. minimum* were 5'–AGG TCG

GGG GCC AAC–3' and 5'–AGG TGT AAA CTA CTG CGC–3', and for the quantification of *Pa. chlamydospora* were 5'–CTC CAA CCC TTT GTT TAT C–3' and 5'–TGA AAG TTG ATA TGG ACC C–3' (Tegli et al. 2000). Real time PCR analyses were performed in an Applied Biosystems StepOnePlus PCR System and for the amplification reactions, Maxima SYBR Green qPCR Master Mix (2X) (Thermoscientific) was used. The results were analyzed with StepOne v.2.3 software. Fungal DNA quantity values were normalized relative to plant DNA based on the grapevine housekeeping gene EF1γ (XM_003633372.1), using the primer pair 5'-GAAGGTTGACCTCTCGGATG -3' and 5'-AGAGCCTCTCCCTCAAAAGG-3'. Two Step PCR cycling started with an initial denaturation at 95 °C for 10 min, followed by 40 cycles of denaturation at 95 °C for 15 s, and an annealing step at 60 °C for 1 min. All samples were tested in triplicates and the experiment was repeated thrice.

Lignin and phenolic compounds quantification in wood tissue

Lignin extraction and quantification was performed according to Schenk and Schikora (2015) and fractions containing cell-wall bound phenolics and soluble phenolics were collected for further quantification using Folin and Ciocalteu (1927) method, with slight modifications. Briefly, to each sample were added 5 volumes of H_2O, equal volume of Folin-Ciocalteu reagent (PanReac AppliChem, Spain) and 4 volumes of Na_2CO_3 (Merck, Germany). Incubation took place for 90 min in the dark and absorbance was measured at 750 nm. All samples were tested in triplicates.

LC-MS untargeted analysis

Untargeted metabolomic analysis was conducted for the hydrolyzed products (LMW-BM), which displayed the most promising antifungal effect *in vitro*. Sample preparation involved a simple 1:30 dilution of the extract with Milli-Q water [offered ultrapure water, 18.2 MΩ·cm (Millipore, Bedford, MA, USA) (20 µL diluted to 600 µL)], followed by filtration through 0.22 µm PTFE syringe filters, and transfer into 2 mL amber LC–MS glass vials. Each experimental group comprised 3 biological replicates, each analyzed in duplicate analytical injection ($N = 2 \times 2$), with both injections retained as separate observations to preserve intra-sample variance information rather than suppressing it through averaging (Glaab and Schneider 2015). For the untargeted analysis an UHPLC–ESI–TIMS–QTOF (Ultra-High Performance Liquid Chromatography coupled to Electrospray Ionization Trapped Ion Mobility Quadrupole Time-of-Flight Tandem Mass Spectrometry) instrument was used. In detail, the samples were analyzed with an Elute PLUS LC series system (Bruker, Bremen, Germany) coupled to the TIMS-TOF Pro 2 (Bruker, Bremen, Germany) mass spectrometer. Chromatographic separation, mass spectrometer acquisition parameters, including source settings, fragmentation conditions, and calibration protocol, were identical to those reported by Arapitsas et al. (2026) method on an Acquity UPLC HSS T3 1.8 µm × 2.1 mm × 100 mm (Waters, Massachusetts). LC-MS data were acquired using DDA (Data-Dependent Acquisition), capturing ions in the range from 20 to 1300 *m/z*. The column oven was set at 40 °C, and the flow was 0.35 mL/min for the 10 µL of injected sample. The injection sequence was randomized using Random.org to minimize instrumental bias.

Statistical analysis and LC-MS data analysis

Data on fungal growth, conidiation, wood discoloration measurements, pathogens' DNA quantification, lignin and phenolic compounds quantification were analyzed by one-way analysis of variance (ANOVA), followed by Dunnett's test for multiple comparisons with the control (P-value < 0.05), using the statistical software Minitab 19.

The acquired liquid chromatography raw spectrometric data were processed using MetaboScape (v2025b) (Pergande et al. 2024). Bucket lists for feature-data collected in positive and negative ionization modes were generated using the T-Rex 4D algorithm using a mass error of ≤5.0 ppm and retention time tolerance of 20 s.

Statistical analysis and data visualization (heatmaps and Principal Components Analysis – PCA- plots) of features was conducted using MetaboAnalyst 6.0 (Montreal, QC, Canada). Prior to statistical analysis, features with near-constant abundance across experimental conditions were removed using an interquartile range filter (IQR < 40th percentile), and data were subjected to Pareto scaling normalization. The biomarkers underwent statistical clustering via Tukey-Kramer HSD pairwise comparisons (JMP 17, Statistical Discovery LLC, Cary, NC). Significant markers were identified through ANOVA (P-value < 0.05) for both ESI+ and ESI− modes, with additional filtering for FDR < 0.05 (Benjamini-Hochberg). Fold change (FC) and log2FC were calculated for strain and fermentation contrasts. A correlation heatmap analysis was performed, on row-wise z-scored intensities, in order to determine the most relevant biomarkers for each of the two pathogen inhibition activities. Finally, putative biomarkers were selected based on intermediate negative correlations ($r < -0.3$) with pathogen growth, and the $r < -0.3$ exploratory threshold was applied consistent with the FDR tolerance used in the upstream ANOVA filtering.

Metabolite annotation adhered to the four-level identification framework proposed by Sumner et al. (2007). Level 1 (identified compounds) required at least two orthogonal parameters obtained under identical conditions (e.g., accurate mass, retention time, MS/MS spectrum, and CCS) matched to authentic standards. Level 2 (putatively annotated compounds) was assigned based on accurate mass and MS/MS spectral similarity against public databases (MassBank, AnalyteList Bruker HMDB Library 2.0, MSDIAL ESI(+)-MS/MS library containing 16,232 authentic standards) and an in-house library, using a mass error $\leq$ 5.0 ppm and retention time deviation $\leq$ 0.5 min. Level 3 (putatively characterized compound classes) was based on diagnostic MS/MS fragmentation patterns and physicochemical properties characteristic of specific metabolite classes. Features that could not be structurally assigned but were consistently detected and quantified were classified as Level 4 (unknown compounds). Manual curation using MetFrag (https://msbi.ipb-halle.de/MetFrag/index.xhtml, accessed on 24 February 2026), and HMDB (https://hmdb.ca/metabolites, accessed on 24 February 2026) was performed for low-confidence matches to improve annotation reliability.

Results

Alcoholic fermentation and production of wine lees

The fermentation kinetics, expressed as CO_2 release (g/L) and the variation in CO_2 production rate, over time is depicted in Online Resource ESM_1, Fig. S1. Alcoholic fermentation was successfully completed in all trials, with durations ranging from 57 to 203 h. Fermentation time was significantly shorter in the *S. cerevisiae* monocultures of both strains compared to the mixed fermentations, and the fermentation rate was also significantly higher. However, no sluggish or stuck fermentations were observed. Additionally, the evolution of the total viable population (TVP) across all fermentation modalities exhibited similar kinetics (Online Resource ESM_1, Fig. S2A), indicating comparable microbial growth patterns among the different inoculation strategies. The dynamics of viable yeast populations (log CFU/mL) of the two species dominating alcoholic fermentation are presented in Online Resource ESM_1, Fig. S2. In the sequential inoculation modalities, the non-*Saccharomyces* population predominated prior to the inoculation of *S. cerevisiae*, actively contributing to the early stages of fermentation. However, within 48 h after the addition of *S. cerevisiae*, *Hanseniaspora* sp. was consistently outcompeted, maintaining approximately a 1 log CFU/mL lower population than the dominant *S. cerevisiae* strain for the remainder of the process (Online Resource ESM_1, Fig. S2B). Despite these population shifts, no significant differences were observed in the overall biomass yield (Online Resource ESM_1, Fig. S3), which ranged from 16.3% to 19.8% (w/v). Consequently, the mixtures produced from wine lees derived from mixed-culture fermentations were expected to differ in chemical composition compared to those obtained from monoculture fermentation schemes, as both inoculated strains were detected at the end of the fermentation process in the lees.

Effect of high and low molecular weight biomolecule mixtures on fungal growth

HMW-BM and LMW-BM mixtures were tested for their antifungal properties against *Pm. minimum* and *Pa. chlamydospora in vitro*. None of the HMW-BM mixtures were able to reduce fungal growth for both fungi (Fig. 2a and b). On the other hand, all LMW-BM mixtures were able to reduce pathogens' growth (Fig. 2a and b). Specifically, LMW-BM S1, S3, S1H and S3H mixtures reduced at 18 dpi *Pm. minimum* growth by 45%, 72%, 57% and 75%, and *Pa. chlamydospora* growth by 40%, 51%, 46% and 57%, respectively.

Effect of high and low molecular weight biomolecule mixtures on fungal sporulation

None of the HMW-BM mixtures affected conidia production at 18 dpi (Fig. 2e and f). On the other hand, LMW-BM mixtures were able to significantly reduce sporulation for both fungi. Sporulation of *Pm. minimum* was significantly restricted by all LMW-BM mixtures except for LMW-BM S1 mixture which displayed a non-statistically significant reduction (Fig. 2e). LMW-BM S3, S1H and S3H mixtures reduced *Pm. minimum* sporulation at 18 dpi by 52%, 56% and 92% respectively. *Pa. chlamydospora* produced less conidia in the presence of all LMW-BM mixtures with the exception of LMW-BM S1H mixture, where the reduction was not statistically significant (Fig. 2f). LMW-BM S1, S3 and S3H mixtures reduced *Pa. chlamydospora* sporulation at 18 dpi by 47%, 43% and 61%, respectively.

Phytoprotective effect of P1 and P2 products and restriction of endophytic fungal growth

Both products, P1 and P2, were able to reduce the wood discoloration caused by *Pm. minimum* and by *Pa. chlamydospora* with a statistically significant difference (Fig. 3a). Products P1 and P2 reduced wood discoloration caused by *Pm. minimum* by 47% and 52%. They also reduced symptoms caused by *Pa. chlamydospora* by 35% and 73% respectively.

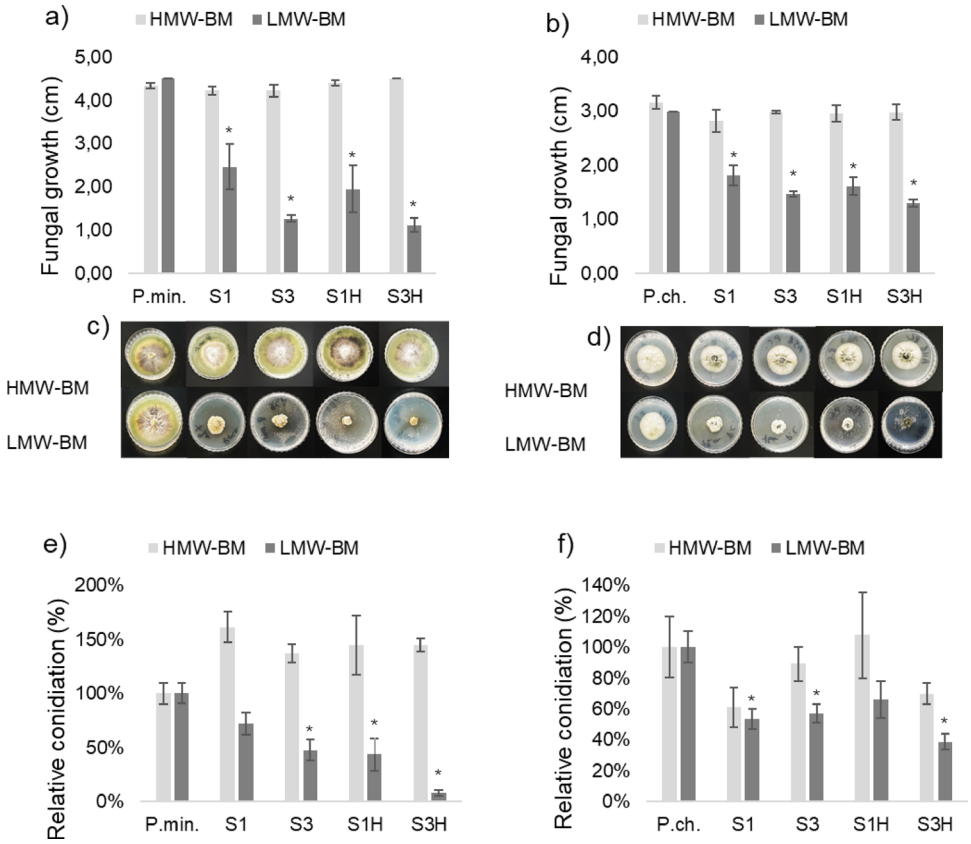

Fig. 2 Fungal growth (**a**, **b**) and relative conidiation (**e**, **f**) in PDA growth medium amended with 10 µg/mL of High Molecular Weight Biomolecules Mixtures (HMW-BM) mixtures (light grey) and Low Molecular Weight Biomolecules Mixtures (LMW-BM) mixtures (dark grey). Fungal growth was recorded 18 dpi for both fungi. All samples were tested in triplicates (3 petri dishes) and the experiment was repeated three times ($n=9$). Columns represent means of the three replications (9 petri dishes) and the vertical bars indicate standard errors. Columns with an asterisk (*) are significantly different from the control, as determined by one-way analysis of variance (ANOVA), followed by Dunnett's test for multiple comparisons with the control (*p-value*<0.05). Photographs of *Pm. minimum* (*P. min.*) (**c**) and *Pa. chlamydospora* (*P. ch.*) (**d**) growth at 18 dpi, treated with HMW-BM mixtures (first row) and LMW-BM mixtures (second row)

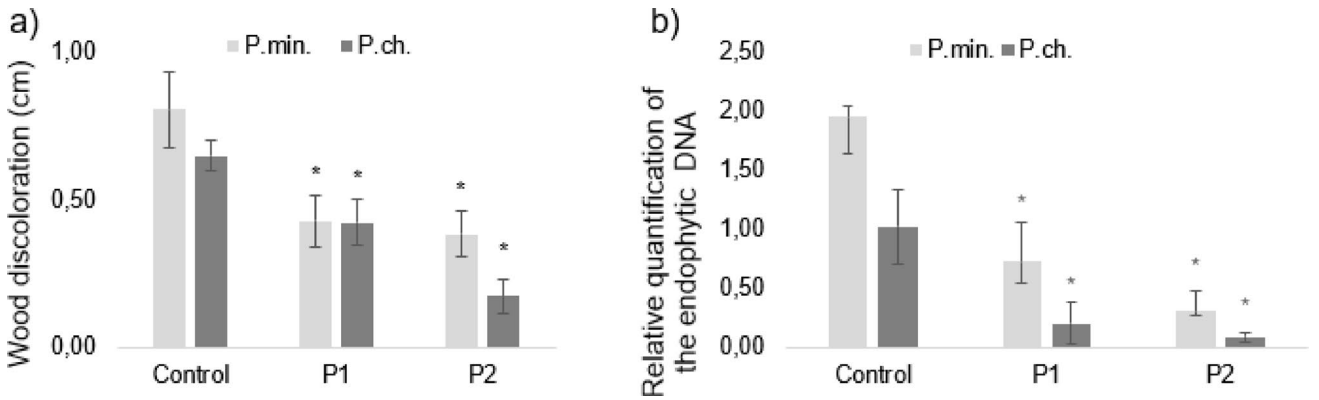

Fig. 3 Length of wood discoloration caused by *Pm. minimum* (P. min.) and *Pa. chlamydospora* (P. ch.) (**a**) at 112 dpi, treated with 10 µg/ml LMW-BM mixtures (P1 and P2). Columns represent the means of three biological replicates with 12 artificially inoculated rooted cuttings per replicate ($n=36$) and the vertical bars indicate standard errors. Columns with an asterisk (*) are significantly different from the control as determined by one-way analysis of variance (ANOVA), followed by Dunnett's test for multiple comparisons with the control (*P*-value <0.05). Relative quantification of the endophytic *Phaeoacremonium minimum* (*P. min.*) DNA and *Phaeomoniella chlamydospora* (*P. ch.*) DNA (**b**) in artificially inoculated rooted cuttings at 112 dpi, treated with P1 and P2 products. Columns represent the means of three biological replicates with 3 artificially inoculated rooted cuttings per replicate ($n=9$) and the vertical bars indicate standard errors. Columns with an asterisk (*) are significantly different from the control, as determined by one-way analysis of variance (ANOVA), followed by Dunnett's test for multiple comparisons with the control (*P*-value<0.05)

Pathogens' DNA relative quantification was performed on mock-inoculated rooted cuttings (negative control), confirming the absence of *Pm. minimum*'s and *Pa. chlamydospora*'s DNA prior to the inoculation (data not shown). The results of the endophytic *Pm. minimum*'s and *Pa. chlamydospora*'s DNA relative quantification indicated that there was a statistically significant reduction of pathogens' DNA in artificially inoculated rooted cuttings treated with products P1 and P2 (Fig. 3b). Specifically, P1 and P2

reduced *Pm. minimum*'s DNA by 63% and 84%, and *Pa. chlamydospora*'s DNA by 80% and 91%, respectively.

Lignin and phenolic compounds quantification

The results of lignin and phenolic compounds quantification showed that there was no statistically significant difference between plants treated with the mixtures and the control (Online Resource ESM_1, Fig. S4).

Metabolomic analysis

Global metabolomic fingerprinting and fermentation-dependent variation

The untargeted LC-MS analysis of the samples registered 3,029 features in ESI+and 858 in ESI-(Online Resource ESM_2), with the PCA plot of Fig. 4a showing the distribution of the samples when all features were used. The first principal component (PC1) appeared to capture a trend in mixed culture fermentation conditions on the right (LMW-BM HS1 and HS3) and monoculture conditions (LMW-BM S1 and S3) on the left. Along the second principal component (PC2), there was a tendency for the separation of the mixtures obtained from *S. cerevisiae* strain S1 (LMW-BM S1 and S1H), which cluster on the positive values of PC2, from the mixtures obtained from *S. cerevisiae* strain S3 (LMW-BM S3 and S3H), which tend to cluster on the negative values of PC2.

Differential metabolite profiling between mono- and mixed-culture fermentations

The heatmap (Fig. 4b) displays a clear separation between monoculture derived (LMW-BM S1 and S3) and mixed culture derived (LMW-BM S1H and S3H) mixtures, confirming that mixed culture fermentations with *Hanseniaspora* sp. were the dominant factor influencing the metabolomic profile. The left cluster, corresponding to monocultures, shows extensive red–blue contrast (red for upregulated and blue for downregulated features).

Statistical discrimination and correlation-based biomarker selection

Following this initial metabolomic profiling, a systematic statistical workflow was applied to identify metabolites associated with antimicrobial activity. ANOVA (P-value < 0.05, FDR < 0.05) revealed 448 significantly discriminant features (Online Resource ESM_3) and varied significantly across fermentation conditions. In monoculture, the two *S. cerevisiae* strains differed in 153 features (34.6% with > 2-fold change), whereas their corresponding mixed cultures differed in only 8 features (1.8%), indicating that although *S. cerevisiae* strain plays an important role in metabolite composition, co-fermentation with *Hanseniaspora* may substantially reduce strain-dependent metabolomic differences. Additionally, 71.7% of features in S1H were more similar to the S1 parent than to S3H, demonstrating strong retention of metabolic fingerprint. To further explore the relationship

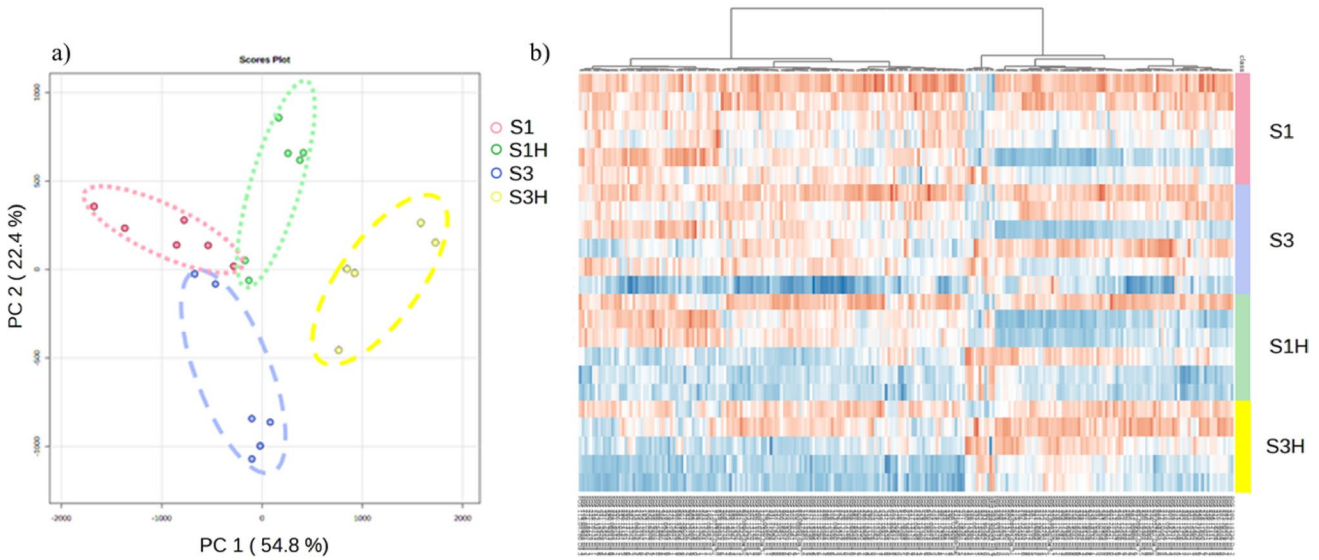

Fig. 4 Principal Component Analysis (PCA) scores plot of pre-filtered metabolomic features (bottom 30% by mean intensity removed) across four sample groups (ESI+and -). S1 (magenta circles), S3 (blue circles), S1H (green circles), and S3H (yellow circles) (**a**), and Heatmap of the top 125 feature (P-value < 0.005) ranked by one-way ANOVA (ESI+and ESI−), with Ward hierarchical clustering applied to features (**b**). Red and blue intensities indicate stronger positive and negative statistical correlations between the sample and the feature. The lateral color represents the classification among different groups S1 (magenta), S3 (blue), S1H (green) and S3H (yellow)

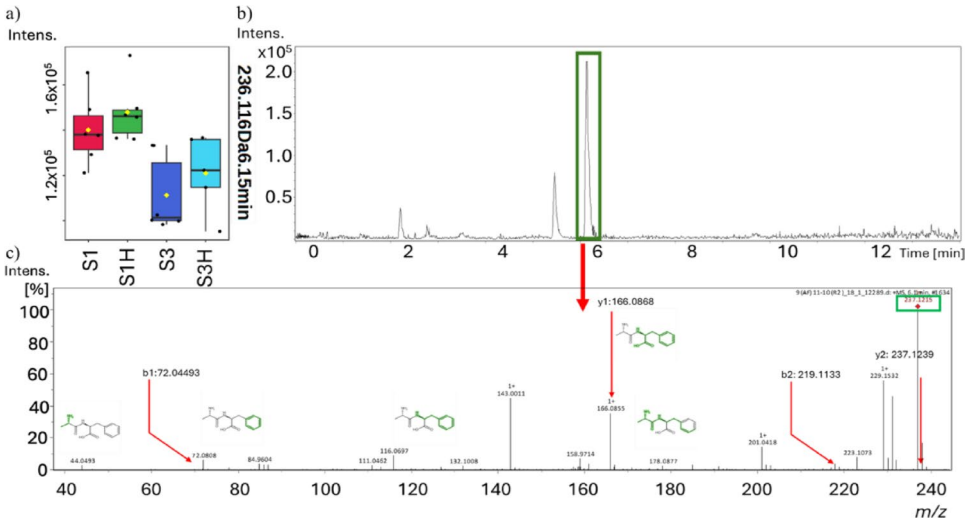

Fig. 5 Characterization of metabolite Ala-Phe: Intensity distribution boxplot (**a**), Precursor ion mass spectrum (*m/z* 236.116 Da) (**b**), and Fragmentation pattern at 6.15 min (**c**)

between metabolite abundance and pathogen development, a hierarchical clustering heatmap was constructed based on Pearson correlation coefficients for both *Pm. minimum* and *Pa. chlamydospora* (Online Resource ESM_1, Fig. S5A and S5B, respectively), enabling the visual identification of features negatively associated with fungal growth.

Features displaying a correlation coefficient $r < -0.3$ were retained for downstream annotation, yielded 49 putative biomarkers showing significant negative correlations with pathogen development (P-value < 0.05, Online Resource ESM_4), which were annotated at confidence levels 1–4, with 2 at level 1, 19 at level 2, 6 at level 3, and 22 at level 4. Most of these markers eluted within a retention time window of (5.0 ± 2.8) min (mean ± SD), a range encompassing the 448 ANOVA-significant features, and exhibited an average molecular mass of approximately (307.5 ± 150) Da (mean ± SD). Among them, 26 out of 49 features (53.1%) were peptide-related, including 20 confirmed peptides at levels 1–2 (one level 1 compound, Glutamylphenylalanine, and 19 level 2 sequence-confirmed di- and tripeptides) and 6 peptide-like compounds at level 3. The remaining 23 features comprised 22 unknowns at level 4 and Proline, the sole identified non-peptide compound.

Physicochemical characterization of putative antifungal metabolites

These low-molecular-weight compounds (Online Resource ESM_5) are in silico characterized at pH 7.4 by a net charge ranging from −1 to +0.5 and isoelectric points (pI) between 3.8 and 7.1. Their steric hindrance values ranged from 0.35 to 0.73, with amphipathic indices between 0 and 1.26 and hydrophobicity values from −0.54 to 0.66, indicating generally low hydrophobicity and moderate polarity. These descriptors are reported as a descriptive overview of the annotated peptide pool to contextualize their properties within the broader framework of antimicrobial peptide research and were not used as selection or ranking criteria among candidate biomarkers. The MS/MS fragmentation pattern (Fig. 5c) confirms its structural assignment, with characteristic fragment ions highlighted in red and the precursor ions in green. Together, these parameters support the structural annotation Ala-Phe as a putative bioactive peptide constituent of the LMW-BM mixtures.

The feature at *m/z* 274.1773 [M+H] Da (6.88 min) shows a negative correlation between its presence with the pathogen growth and conidia production across all post-inoculation timepoints of the study, and was tentatively identified as the tripeptide Ile-Ala-Ala (annotation level 2). Among the discriminant metabolites, Glu-Gln, Ile-Ser-Ala, and Glutamylphenylalanine were upregulated in LMW-BM S1 and S1H and downregulated in LMW-BM S3 and S3H mixtures, suggesting differences in peptide hydrophobicity due to the differences between retention time and charge distribution that may underlie the observed strain-dependent bioactivity.

The feature tentatively identified as Ile-Ala-Ala (annotated at 273.1688 *m/z* [M], 6.88 min), showed based on correlation analysis, the strongest negative association with pathogen growth among the putative biomarkers identified, with inhibition of mycelial growth and conidial production on *Pm. minimum* (r = −0.54 and −0.42, respectively) and *Pa. chlamydospora* mycelial growth (r = -0.46), suggesting it is a candidate compound of interest for future experimental validation. Its prioritization over other annotated peptides was based exclusively on these correlation values. Its physicochemical properties were characterized in silico (pH = 7.4) with a total charge of 0, pI of 5.88, steric hindrance of 0.58, and hydrophobicity of 0.41. One possible interpretation, aligned with models for antimicrobial peptides, is that this compound may function by interacting with the pathogen's membrane.

Structural annotation of putative bioactive molecules

The analytical characterization of proposed annotated bioactive molecules based on correlation analyses is illustrated in Fig. 5 by the feature *m/z* 236.1161 (observed $[M+H]^+$ = 237.1273) eluting at 6.15 min tentatively annotated at confidence level 2 as the dipeptide Ala-Phe (alanyl-phenylalanine). This annotation reflects structural identification based on accurate mass and MS/MS spectral matching; it does not constitute direct evidence of biological activity, which is addressed separately through the correlation analysis (ESM_4). In Fig. 5a, its relative abundance was highest in LMW-BM S1H, followed by S1 and S3, while it was minimal in S3H, suggesting a strain- and mixed-culture-dependent formation. The extracted ion chromatogram and mass spectrum (Fig. 5b) display a distinct precursor ion at *m/z* 237.1273 eluting at 6.15 min. The MS/MS spectrum (Fig. 5c) confirms the Ala-Phe sequence through complementary N- and C-terminal sequence ions, including a1 (*m/z* 44.049), b1 (*m/z* 72.045), b2 (m/z 219.113), and y1 (*m/z* 166.087), the most abundant fragment ion. The convergence of these a-, b-, and y-ions spanning both termini provides robust structural support for this assignment. Ala-Phe was selected as a representative example based on two criteria: its significant negative correlation with pathogen development and the completeness of its MS/MS fragmentation pattern among the annotated dipeptide constituents of the LMW-BM fractions.

Discussion

Several biomolecules, such as peptides with antimicrobial activity have been produced, isolated and purified from different sources such as microorganisms, invertebrates and other species (Liu et al. 2007; Alfonzo et al. 2012; Lachhab et al. 2016; Yang et al. 2023). Yeast-derived peptides from spent brewer's yeast (*S. cerevisiae) h*ave demonstrated antimicrobial activity against bacteria and fungi (Oliveira et al. 2022). Wine lees mainly consist of dead yeast cells (De Iseppi et al. 2020) which makes them a source of potential yeast-derived antimicrobial peptides which could be valuable in plant protection. Therefore, this work focused on upgrading wine lees into biomolecule mixtures containing secondary metabolites and peptide-related compounds with potential antimicrobial activity.

None of the HMW-BM mixture was able to reduce fungal growth for both fungi *in vitro*. On the other hand, all LMW-BM mixtures were able to reduce pathogens' growth for both fungi, indicating that enzymatic hydrolysis of proteins is an essential step to generate low-molecular weight bioactive fractions with antimicrobial potential. Although FAN confirmed the successful generation of low-molecular-weight nitrogenous compounds after hydrolysis, there was no clear association between FAN concentration and antifungal efficacy. The four LMW-BM fractions exhibited very similar FAN values ($P>0.05$), while their antifungal activities differed considerably, suggesting that bioactivity is more likely related to the qualitative composition of the low-molecular-weight fractions. To the best of our knowledge, only one study using peptides derived from *Bacillus amyloliquefaciens* proteins shows an *in vitro* antifungal activity against *Pa. chlamydospora*, *Pm. minimum*, and also against *Botrytis cinerea* and *Aspergillus carbonarius*, two grapevine pathogens which are also ascomycete fungi (Alfonzo et al. 2012), However, several peptides, such as synthetic peptides (Fan et al. 2023, 2024), peptides obtained from marine sources (Liu et al. 2007; Yang et al. 2023), commercial peptides derived from lupin (Monteiro et al. 2015; Lachhab et al. 2016), soybean, casein (Lachhab et al. 2016), or whey (Alfonso et al. 2025), have been demonstrated to reduce fungal growth or plant symptoms caused by *B. cinerea*. A *Bacillus subtilis* tryptic hydrolysate restricted *Aspergillus niger* growth, also an ascomycete, *in vitro* (Zhang et al. 2018).

Previous studies with several ascomycetes have shown that the antifungal activity of peptides can be strongly influenced by their physicochemical properties, particularly charge, isoelectric point, steric hindrance, amphipathicity, hydrophobicity, and secondary structure, which govern their interactions with microbial cells (Sagan et al. 2003; Mookherjee and Hancock 2007; Chen et al. 2021; Allen and Pellois 2022; Brango-vanegas et al. 2024). Cationic peptides with net positive charge (+2 to +9) can bind to anionic phospholipids in fungal membranes, forming pores and causing membrane lysis (Marcos et al. 2008). It should be noted, however, that most putative biomarkers identified in this study present physicochemical properties that differ from those typically associated with well-characterized cationic antimicrobial peptides, such as low net charge (ranging from −1 to +0.5) and moderate hydrophobicity. Putative structure–activity relationships, based on tentative annotations, may offer a preliminary explanation for the observed differences in antifungal activity associated with smaller peptides, such as those detected in LMW-BM mixtures, showing greater activity (Albuquerque and Casadevall 2012). Low hydrophobicity and electrostatic interactions could possibly be promoted by some of those compounds, damaging surface fungal cells in a carpet or electroporation model, facilitating the translocation of the peptide across the membrane to reach an intracellular target, as described by Gan et al. (2021). This explanation provides a basis to understand the inhibition of pathogens using small protein lysates with low hydrophobicity and electrostatic charge.

Other possible mechanisms that could hypothetically be involved include inhibition of cell wall synthesis through interactions with chitin and β-glucan synthases (De Cesare et al. 2020), metal chelation by cysteine- or histidine-rich motifs, fungal hyphae deformation (Sóvágó et al. 2012), decrease of mitochondrial membrane potential and mitochondrial related enzyme activities, oxidative stress (Wang et al. 2019; Fan et al. 2023; Yang et al. 2023), and biofilm destabilization via binding to extracellular DNA and polysaccharides (Segev-Zarko et al. 2015). Low molecular weight biomolecules may also interfere with fungal quorum sensing or modulate gene expression linked to membrane metabolism and DNA replication (Fan et al. 2024).

The reduction in sporulation by LMW-BM mixtures could possibly be linked to peptide-mediated interference with fungal developmental processes, potentially through membrane destabilization, disruption of mitochondrial function, oxidative stress induction, or interference with quorum sensing pathways involved in conidiation as suggested by previous studies (Segev-Zarko et al. 2015; Fan et al. 2023).

In vivo experiments in artificially inoculated rooted cuttings showed that the low-molecular-weight bioactive fractions were effective at reducing symptoms (wood discoloration) caused by the two pathogens and reducing internal pathogen colonization. To further investigate the possibility of plant defense mechanism activation, lignin and phenolic compounds quantification was conducted, but the results did not provide evidence that the biomolecule mixtures used in this study activated the plant defence mechanism involving lignification or phenolic compounds, either cell wall bound or soluble (Bhuiyan et al. 2009; Bhattacharya et al. 2010).The metabolomic fingerprint of LMW-BM mixtures revealed strain- and fermentation-dependent differences, highlighting the influence of yeast interactions on the composition of nitrogenous compounds. Fermentations with *Saccharomyces* strains alone promoted the accumulation of a broad range of metabolites. In contrast, mixed culture fermentations with *Hanseniaspora* sp. resulted in a general downregulation of putative peptide and small-molecule features, suggesting metabolomic reprogramming under mixed fermentation conditions. Both the yeast strain and its interaction with *Hanseniaspora* sp. jointly shaped the final metabolomic fingerprint, as supported by the partial group separation observed in the PCA and the hierarchical clustering pattern in the heatmap, where neither factor alone drove a clean separation between groups. The different metabolomic profiles of LMW-BM fractions based on the fermentation schemes along with their effectiveness in reducing fungal growth and conidiation indicate that strain- and fermentation-dependent peptide profiles may influence antifungal activity. Our results indicate the tripeptide Ile-Ala-Ala (annotated at 273.1688 *m/z* [M], 6.88 min) was the candidate biomarker most strongly negatively associated with mycelial growth for both pathogens, and conidial production for *Pm. minimum*. Specifically, the correlation for *Pm. minimum*'s mycelial growth and conidiation were −0.54 and −0.42, respectively. Considering *Pa. chlamydospora*, the correlation in mycelial growth was −0.46. The tripeptide Ile-Ala-Ala was characterized in silico (pH = 7.4) with a total charge of 0, pI of 5.88, steric hindrance of 0.58, and hydrophobicity of 0.41.

Conclusion

This study shows that a carefully managed, integrated bioprocess can convert wine lees—an abundant winery waste—into bioactive fractions with notable antifungal activity against key grapevine pathogens. The lack of activity in high-molecular-weight autolysates, along with the consistent inhibition of mycelial growth and conidiation for both *Pm. minimum* and *Pa. chlamydospora* by all low-molecular-weight fractions, highlights enzymatic hydrolysis and membrane fractionation as important steps for generating low-molecular-weight bioactive fractions, such as peptides, with antimicrobial activity. In addition to the *in vitro* findings, *in vivo* phytoprotection tests confirmed that soil application of the combined low-molecular-weight products significantly reduced wood discoloration and limited endophytic pathogen colonization in grapevine rooted cuttings. Nevertheless, additional experiments should be conducted in order to evaluate the products' effectiveness under field conditions, since their efficacy and stability could be affected by several variables such as products' concentration, soil consistency, UV radiation, temperature and weather conditions. Untargeted UHPLC–ESI–TIMS–QTOF metabolomics provided activity-linked fingerprinting, indicating that the observed antifungal activity is likely influenced by strain- and fermentation-dependent low-molecular-weight metabolite profiles, including peptide-related compounds. Within this profile, the tripeptide Ile-Ala-Ala emerged as the putative biomarker with the strongest negative correlation with pathogen growth, representing a priority candidate for future isolation and bioassay validation, while acknowledging that its causal role remains to be experimentally confirmed. These results demonstrate that fermentation design can be a controlled upstream quality factor within a scalable, circular-economy-oriented valorization process. Future research should explore potential synergistic effects among the identified compounds, improve structure–activity understanding, and evaluate field applications to facilitate the adoption of sustainable viticulture practices.

Supplementary Information The online version contains supplementary material available at https://doi.org/10.1007/s43393-026-00539-4.

Acknowledgements The authors wish to thank Professors Epameinondas J. Paplomatas and Sotirios E. Tzamos for providing the pathogen strains from the collection of the Laboratory of Plant Pathology of the Agricultural University of Athens.

Author contributions A.T. : investigation, data curation, methodology, formal analysis, validation, visualization, writing-original draft, writing—review and editing, P.-G. G.: conceptualization, investigation, data curation, methodology, formal analysis, validation, visualization, writing-original draft, writing—review and editing, A.K.: investigation, data curation, methodology, formal analysis, validation, visualization, writing-original draft, writing—review and editing, A.T. : investigation, data curation, methodology, formal analysis, validation, visualization, writing-original draft, writing—review and editing, G.N.: investigation, methodology, resources, visualization, writing—review and editing A.E.: conceptualization, methodology, project administration, resources, supervision, writing—review and editing, C.V.: supervision, writing—review and editing, G.T: supervision, writing—review and editing, . M.D.: conceptualization, funding acquisition, investigation, data curation, methodology, project administration, resources, supervision, validation, writing-original draft writing—review and editing, P.A.: conceptualization, funding acquisition, data curation, methodology, project administration, resources, supervision, visualization, writing-original draft, writing—review and editing, D.G.: conceptualization, investigation, data curation, methodology, project administration, resources, supervision, validation, writing-original draft, writing—review and editing.

Funding Open access funding provided by Fondazione Edmund Mach - Istituto Agrario di San Michele all'Adige within the CRUI-CARE Agreement. The research project is implemented in the framework of the H.F.R.I. call “Basic research Financing (Horizontal support of all Sciences)” under the National Recovery and Resilience Plan “Greece 2.0” funded by the European Union—NextGenerationEU (Hellenic Foundation for Research and Innovation Project Number: 15100).

Data availability The datasets generated during and/or analysed during the current study are available in the Supplementary Material.

Declarations

Competing interests The authors declare no competing interests.

References

Akbarian M, Khani A, Eghbalpour S, Uversky VN. Bioactive Peptides: Synthesis, Sources, Applications, and Proposed Mechanisms of Action. Int J Mol Sci. 2022;23:1445. https://doi.org/10.3390/ijms23031445.

Albuquerque P, Casadevall A. Quorum sensing in fungi a review. Med Mycol. 2012;50:337–45. https://doi.org/10.3109/13693786.2011.652201.

Alfonso E, Andlauer W, Brück WM, Rienth M. Whey protein hydrolysates enhance grapevine resilience to abiotic and biotic stresses. Front Plant Sci. 2025;16:1521275. https://doi.org/10.3389/fpls.2025.1521275.

Alfonzo A, Lo Piccolo S, Conigliaro G, et al. Antifungal peptides produced by Bacillus amyloliquefaciens AG1 active against grapevine fungal pathogens. Ann Microbiol. 2012;62:1593–9. https://doi.org/10.1007/s13213-011-0415-2.

Allen J, Pellois JP. Hydrophobicity is a key determinant in the activity of arginine – rich cell penetrating peptides. Sci Rep. 2022;12:15981. https://doi.org/10.1038/s41598-022-20425-y.

Arapitsas P, Marinaki M, Virgiliou C, Theodoridis G. Untargeted metabolomics reveals key biochemical shifts during industrial Muscat of Alexandria alcoholic fermentation. Food Chem. 2026;506:148090. https://doi.org/10.1016/j.foodchem.2026.148090.

Bérdy J. Bioactive Microbial Metabolites. J Antibiot. 2005;58:1–26. https://doi.org/10.1038/ja.2005.1.

Bhattacharya A, Sood P, Citovsky V. The roles of plant phenolics in defence and communication during Agrobacterium and Rhizobium infection. Mol Plant Pathol. 2010;11:705–19. https://doi.org/10.1111/j.1364-3703.2010.00625.x.

Bhuiyan NH, Selvaraj G, Wei Y, King J. Role of lignification in plant defense. Plant Signal Behav. 2009;4:158–9. https://doi.org/10.4161/psb.4.2.7688.

Bordiga M (2016) Valorization of wine making by-products., 1st editio.

Bradford MM. A rapid and sensitive method for the quantitation of microgram quantities of protein utilizing the principle of protein-dye binding. Anal Biochem. 1976;72:248–54. https://doi.org/10.1016/0003-2697(76)90527-3.

Brango-vanegas J, Leite ML, Macedo MLR, et al. Capping motifs in antimicrobial peptides and their relevance for improved biological activities. Front Chem. 2024;12:1382954. https://doi.org/10.3389/fchem.2024.1382954.

Chen EH-L, Weng C-W, Li M-Y, et al. De Novo Design of Antimicrobial Peptides With a Special Charge Pattern and Their Application in Combating Plant Pathogens. Front Plant Sci. 2021;12:753217. https://doi.org/10.3389/fpls.2021.753217.

Christopoulou M, Tsoukas C, Gkizi D, et al. Development of a molecular diagnostic to discriminate between Fomitiporia species and advancements in detection of the main grapevine decline-related pathogens in propagating material and mature vines. Plant Pathol. 2024;73:326–41. https://doi.org/10.1111/ppa.13812.

Colombo M, Masiero S, Rosa S, et al. NoPv1: a synthetic antimicrobial peptide aptamer targeting the causal agents of grapevine downy mildew and potato late blight. Sci Rep. 2020;10:17574. https://doi.org/10.1038/s41598-020-73027-x.

Das D, Khan T, Kalita J, et al. Antimicrobial peptides: emerging next-generation strategy for sustainable plant disease management. Front Antibiot. 2026;5:1–19. https://doi.org/10.3389/frabi.2026.1766594.

De Cesare GB, Cristy SA, Garsin DA, Lorenz MC. Antimicrobial peptides: A new frontier in antifungal therapy. MBio. 2020;11:e88145. https://doi.org/10.1128/mBio.02123-20.

De Iseppi A, Lomolino G, Marangon M, Curioni A. Current and future strategies for wine yeast lees valorization. Food Res Int. 2020;137:109352. https://doi.org/10.1016/j.foodres.2020.109352.

del Pilar Martínez-Diz M, Díaz-Losada E, Andrés-Sodupe M, et al. Field evaluation of biocontrol agents against black-foot and Petri diseases of grapevine. Pest Manag Sci. 2021;77:697–708. https://doi.org/10.1002/ps.6064.

Deravel J, Lemière S, Coutte F, et al. Mycosubtilin and surfactin are efficient, low ecotoxicity molecules for the biocontrol of lettuce downy mildew. Appl Microbiol Biotechnol. 2014;98:6255–64. https://doi.org/10.1007/s00253-014-5663-1.

Dukes BC, Butzke CE. Rapid Determination of Primary Amino Acids in Grape Juice Using an o-Phthaldialdehyde/N-Acetyl-L-Cysteine Spectrophotometric Assay. Am J Enol Vitic. 1998;49:125–34. https://doi.org/10.5344/ajev.1998.49.2.125.

Fan L, Wei Y, Chen Y, et al. Epinecidin-1, a marine antifungal peptide, inhibits Botrytis cinerea and delays gray mold in postharvest peaches. Food Chem. 2023;403:134419. https://doi.org/10.1016/j.foodchem.2022.134419.

Fan L, Wei Y, Chen Y, et al. Transcriptome analysis reveals the mechanism of antifungal peptide epinecidin-1 against Botrytis cinerea by mitochondrial dysfunction and oxidative stress. Pestic Biochem Physiol. 2024;202:105932. https://doi.org/10.1016/j.pestbp.2024.105932.

Folin O, Ciocalteu V. Tyrosine and Tryptophane in Proteins. J Biol Chem. 1927;73:627–50. https://doi.org/10.1016/S0021-9258(18)84277-6.

Gan BH, Gaynord J, Rowe SM, et al. The multifaceted nature of antimicrobial peptides: Current synthetic chemistry approaches and future directions. Chem Soc Rev. 2021;50:7820–80. https://doi.org/10.1039/d0cs00729c.

Gkikas F, Tako A, Gkizi D, et al. Paenibacillus alvei K165 and Fusarium oxysporum F2: Potential Biocontrol Agents against Phaeomoniella chlamydospora in Grapevines. Plants. 2021;10:207.

Glaab E, Schneider R. RepExplore: Addressing technical replicate variance in proteomics and metabolomics data analysis. Bioinformatics. 2015;31:2235–7. https://doi.org/10.1093/bioinformatics/btv127.

Gramaje D, Úrbez-Torres JR, Sosnowski MR. Managing grapevine trunk diseases with respect to etiology and epidemiology: Current strategies and future prospects. Plant Dis. 2018;102:12–39. https://doi.org/10.1094/PDIS-04-17-0512-FE.

Jang WS, Kim HK, Lee KY, et al. Antifungal activity of synthetic peptide derived from halocidin, antimicrobial peptide from the tunicate, Halocynthia aurantium. FEBS Lett. 2006;580:1490–6. https://doi.org/10.1016/j.febslet.2006.01.041.

Lachhab N, Sanzani SM, Bahouaoui MA, et al. Effect of some protein hydrolysates against gray mould of table and wine grapes. Eur J Plant Pathol. 2016;144:821–30. https://doi.org/10.1007/s10658-015-0749-x.

Liu Z, Zeng M, Dong S, et al. Effect of an antifungal peptide from oyster enzymatic hydrolysates for control of gray mold (Botrytis cinerea) on harvested strawberries. Postharvest Biol Technol. 2007;46:95–8. https://doi.org/10.1016/j.postharvbio.2007.03.013.

Marcos JF, Muñoz A, Pérez-Payá E, et al. Identification and rational design of novel antimicrobial peptides for plant protection. Annu Rev Phytopathol. 2008;46:273–301. https://doi.org/10.1146/annurev.phyto.121307.094843.

Monteiro S, Carreira A, Freitas R, et al. A nontoxic polypeptide oligomer with a fungicide potency under agricultural conditions which is equal or greater than that of their chemical counterparts. PLoS ONE. 2015;10:e0122095.

Mookherjee N, Hancock REW. Cationic host defence peptides: Innate immune regulatory peptides as a novel approach for treating infections. Cell Mol Life Sci. 2007;64:922–33. https://doi.org/10.1007/s00018-007-6475-6.

Niculescu VC, Ionete RE. An Overview on Management and Valorisation of Winery Wastes. Appl Sci. 2023;13:5063. https://doi.org/10.3390/app13085063.

Ntourtoglou G, Tzamourani A, Kasioura A, et al. Efficient Yeast Inactivation and Protein Extraction from Wine Lees Using Pulsed Electric Fields and Ultrasound: A Comparative Energy-Based Approach. Appl Sci. 2025;15:1–12. https://doi.org/10.3390/app15189860.

Oliveira AS, Ferreira C, Pereira JO, et al. Spent brewer's yeast (Saccharomyces cerevisiae) as a potential source of bioactive peptides: An overview. Int J Biol Macromol. 2022;208:1116–26. https://doi.org/10.1016/j.ijbiomac.2022.03.094.

Pergande MR, Osterbauer KJ, Buck KM, et al. Mass Spectrometry-Based Multiomics Identifies Metabolic Signatures of Sarcopenia in Rhesus Monkey Skeletal Muscle. J Proteome Res. 2024;23:2845–56. https://doi.org/10.1021/acs.jproteome.3c00474.

Pons-Mercadé P, Anguela S, Giménez P, et al. Measuring the oxygen consumption rate of some inactivated dry yeasts: Comparison with other common wine antioxidants. Oeno One. 2021;55:147–58. https://doi.org/10.20870/oeno-one.2021.55.2.4618.

Rollero S, Roberts S, Bauer FF, Divol B. Agitation impacts fermentation performance as well as carbon and nitrogen metabolism in Saccharomyces cerevisiae under winemaking conditions. Aust J Grape Wine Res. 2018;24:360–7. https://doi.org/10.1111/ajgw.12338.

Romero D, De Vicente A, Rakotoaly RH, et al. The iturin and fengycin families of lipopeptides are key factors in antagonism of Bacillus subtilis toward Podosphaera fusca. Mol Plant-Microbe Interact. 2007;20:430–40. https://doi.org/10.1094/MPMI-20-4-0430.

Sagan S, Milcent T, Ponsinet R, et al. Structural and biological effects of a b2 - or b3 -amino acid insertion in a peptide. Application to molecular recognition of substance P by the neurokinin-1 receptor. Eur J Biochem. 2003;270:939–49. https://doi.org/10.1046/j.1432-1033.2003.03456.x.

Sanchez-Vallet A, Ramos B, Bednarek P, et al. Tryptophan-derived secondary metabolites in Arabidopsis thaliana confer non-host resistance to necrotrophic Plectosphaerella cucumerina fungi. Plant J. 2010;63:115–27. https://doi.org/10.1111/j.1365-313X.2010.04224.x.

Schenk ST, Schikora A. Lignin Extraction and Quantification, a Tool to Monitor Defense Reaction at the Plant Cell Wall Level. Bio-protocol. 2015;5:e1430. https://doi.org/10.21769/BioProtoc.1430.

Segev-Zarko L, Saar-Dover R, Brumfeld V, et al. Mechanisms of biofilm inhibition and degradation by antimicrobial peptides. Biochem J. 2015;468:259–70. https://doi.org/10.1042/BJ20141251.

Sóvágó I, Kállay C, Várnagy K. Peptides as complexing agents: Factors influencing the structure and thermodynamic stability of peptide complexes. Coord Chem Rev. 2012;256:2225–33. https://doi.org/10.1016/j.ccr.2012.02.026.

Sumner LW, Amberg A, Barrett D, et al. Proposed minimum reporting standards for chemical analysis Chemical Analysis Working Group (CAWG) Metabolomics Standards Initiative (MSI). Metabolomics. 2007;3:211–21. https://doi.org/10.1007/s11306-007-0082-2.

Sun C, Zhao X, Jiao Z, et al The antimicrobial peptide AMP-17 derived from musca domestica inhibits biofilm formation and eradicates mature biofilm in candida albicans. Antibiotics. 2022. . https://doi.org/10.3390/antibiotics11111474.

Tegli S, Bertelli E, Surico G. Sequence analysis of ITS ribosomal DNA in five Phaeoacremonium species and development of a PCR-based assay for the detection of P. chlamydosporum and P. aleophilum in grapevine tissue. Phytopathol Mediterr. 2000;39:134–49. https://doi.org/10.14601/Phytopathol_Mediterr-1555.

Tsioka A, Psilioti Dourmousi K, Poulaki EG, et al. Biocontrol strategies against Botrytis cinerea in viticulture: evaluating the efficacy and mode of action of selected winemaking yeast strains. Lett Apllied Micrbiology. 2024. https://doi.org/10.1093/lambio/ovae026

Tzamourani AP, Taliadouros V, Paraskevopoulos I, Dimopoulou M. Developing a novel selection method for alcoholic fermentation starters by exploring wine yeast microbiota from Greece. Front Microbiol. 2023;14:1–14. https://doi.org/10.3389/fmicb.2023.1301325.

Tzamourani A, Bely M, Thibon C, et al Enhancing the aromatic profile and sensory properties of wine via interactions between Zygosaccharomyces bailii and Saccharomyces cerevisiae. Food Microbiol. 2026. https://doi.org/10.1016/j.fm.2025.104902.

Wang C, Yuan S, Zhang W, et al. Buckwheat Antifungal Protein with Biocontrol Potential to Inhibit Fungal (Botrytis cinerea) Infection of Cherry Tomato. J Agric Food Chem. 2019;67:6748–56. https://doi.org/10.1021/acs.jafc.9b01144.

Yang X, Wang Y, Jiang H, et al. Antimicrobial peptide CB-M exhibits direct antifungal activity against Botrytis cinerea and induces disease resistance to gray mold in cherry tomato fruit. Postharvest Biol Technol. 2023;196:112184. https://doi.org/10.1016/j.postharvbio.2022.112184.

Zhang B, Wang J, Ning S, et al. Peptides derived from tryptic hydrolysate of Bacillus subtilis culture suppress fungal spoilage of table grapes. Food Chem. 2018;239:520–8. https://doi.org/10.1016/j.foodchem.2017.06.153.